

XATOM: an integrated toolkit for X-ray and atomic physics

Sang-Kil Son¹ and Robin Santra^{1,2}

¹CFEL, DESY / ²Department of Physics, University of Hamburg

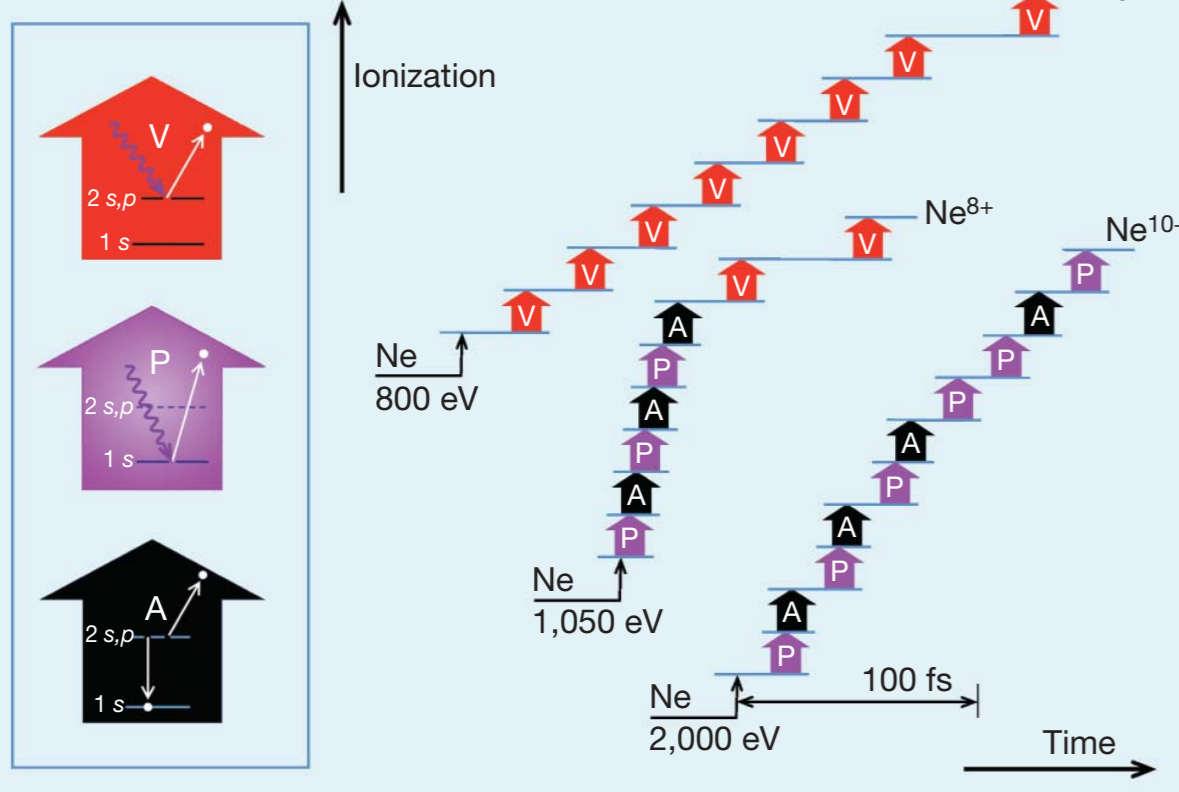


Introduction

X-ray free-electron lasers (XFEL) open a new era in science and technology, offering many possibilities that have not been conceivable with conventional light sources. Because of their very high fluence within very short pulse duration, materials interacting with XFEL undergo significant radiation damage and possibly become highly ionized. To comprehend underlying physics, it is crucial to understand detailed ionization and relaxation dynamics in individual atoms during XFEL pulses. Here we present an integrated toolkit to investigate X-ray-induced atomic processes and to simulate electronic damage dynamics. This toolkit can easily handle all possible electronic configurations of all atom/ion species, and calculate physical observables during/after intense X-ray pulses. It has been successfully applied to study many XFEL-related phenomena from multiphoton ionization to molecular imaging.

Diagrams of multiphoton absorption mechanisms in Ne induced by ultraintense X-ray pulses

Figure from Young *et al.*, *Nature* 466, 56 (2010).



Theoretical and numerical details

Hartree-Fock-Slater model

To treat X-ray-atom interactions, we employ a consistent *ab initio* framework based on nonrelativistic quantum electrodynamics and perturbation theory. For implementation, we use the Hartree-Fock-Slater model, which employs a local density approximation to the exact exchange interaction, with the Latter tail correction.

$$\left[-\frac{1}{2}\nabla^2 + V(\mathbf{r})\right]\psi(\mathbf{r}) = \varepsilon\psi(\mathbf{r}), \text{ where } V(\mathbf{r}) = \begin{cases} -\frac{Z}{r} + \int \frac{\rho(\mathbf{r}')}{|\mathbf{r}-\mathbf{r}'|} d^3r' - \frac{3}{2} \left[\frac{3}{\pi}\rho(\mathbf{r})\right]^{1/3} \\ -\frac{Z - N_{\text{elec}} + 1}{r} \text{ for } r \rightarrow \infty \end{cases}$$

P Photoabsorption

$$\sigma_P(i, \omega) = \frac{4}{3} \alpha^3 \omega N_i \sum_{l_j=|l_i-1|}^{l_i+1} \frac{l_j}{2l_i+1} \left| \int_0^\infty P_{n_i l_i}(r) P_{n_j l_j}(r) r dr \right|^2$$

A Auger decay

$$\Gamma_A(i, j, j') = \pi \frac{N_H^i N_H^{j'}}{2l_i + 1} \sum_{L=|l_j-l_{j'}|}^{l_j+l_{j'}} \sum_{l_p} \sum_{l_r} (2L+1)(2S+1) |M_{LS}(j, j', i, i')|^2$$

F Fluorescence

$$\Gamma_F(i, j) = \frac{4}{3} \alpha^3 (I_i - I_j) \frac{N_H^i N_H^j}{4l_j + 2} \frac{l_j}{2l_i + 1} \left| \int_0^\infty P_{n_i l_i}(r) P_{n_j l_j}(r) r dr \right|^2$$

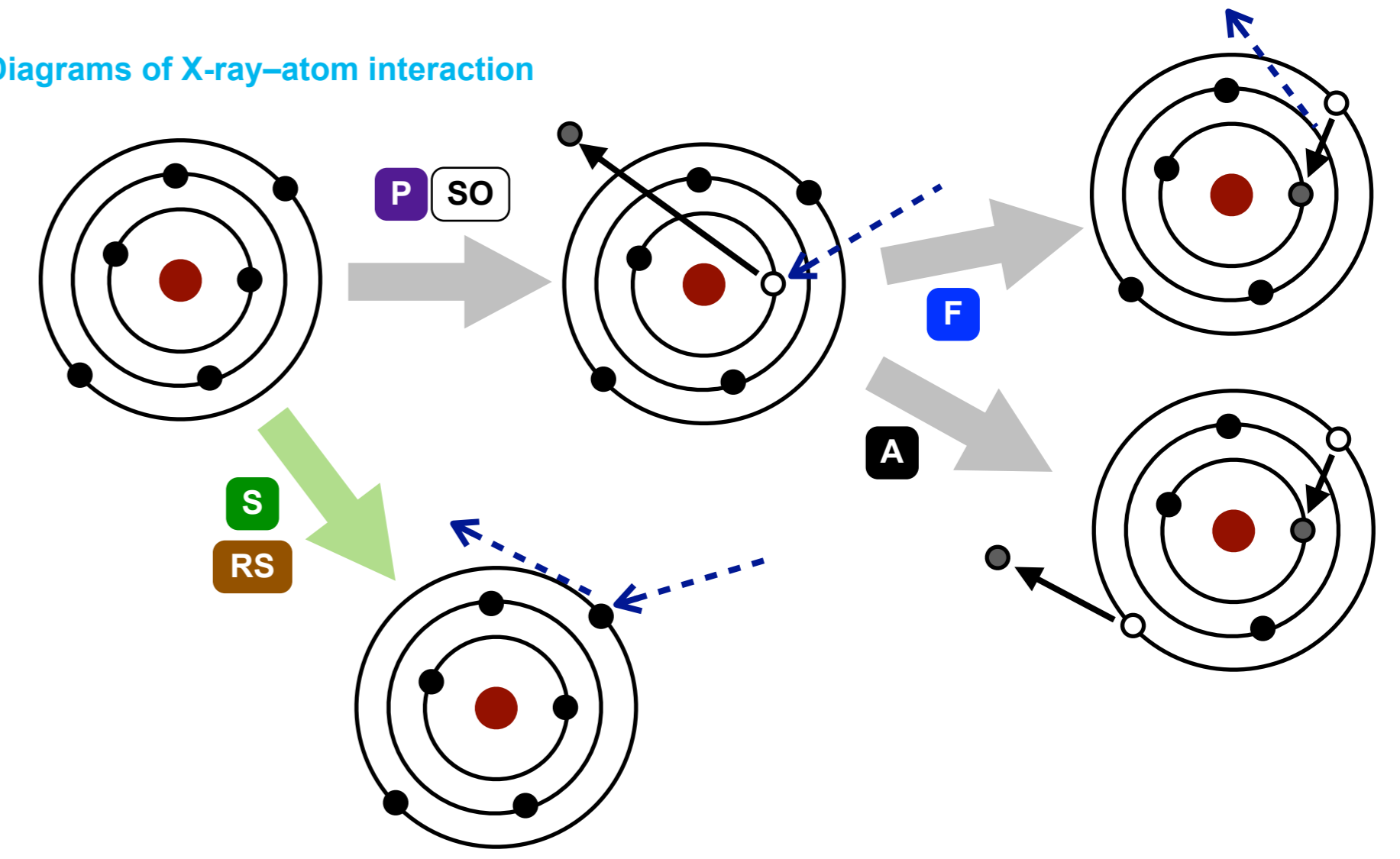
SO Shake-off process

$$ps(i; I, I') = 1 - \left| \int_0^\infty P_{n_i l_i}(r; I) P_{n_i l_i}(r; I') dr \right|^2$$

Rate equation model

$$\frac{d}{dt} P_i(t) = \sum_{i' \neq i}^{\text{all config.}} [\Gamma_{i' \rightarrow i} P_{i'}(t) - \Gamma_{i \rightarrow i'} P_i(t)]$$

Diagrams of X-ray-atom interaction



S Coherent X-ray scattering

$$f^0(\mathbf{Q}) = \int \rho(\mathbf{r}) e^{i\mathbf{Q}\cdot\mathbf{r}} d^3r$$

$$\frac{d\sigma_S}{d\Omega}(t) = \sum_i^{\text{all config.}} P_i(t) \frac{d\sigma_S}{d\Omega}_i = \left(\frac{d\sigma}{d\Omega} \right)_T \sum_i^{\text{all config.}} P_i(t) |f_i^0(\mathbf{Q})|^2$$

RS Resonant elastic X-ray scattering (dispersive correction)

$$f(\mathbf{Q}, \omega) = f^0(\mathbf{Q}) + f'(\omega) + i f''(\omega)$$

$$f'(\omega) = -\frac{1}{2\pi^2 \alpha} \mathcal{P} \int_0^\infty \frac{\omega'^2}{\omega'^2 - \omega^2} \sigma_P(\omega') d\omega'$$

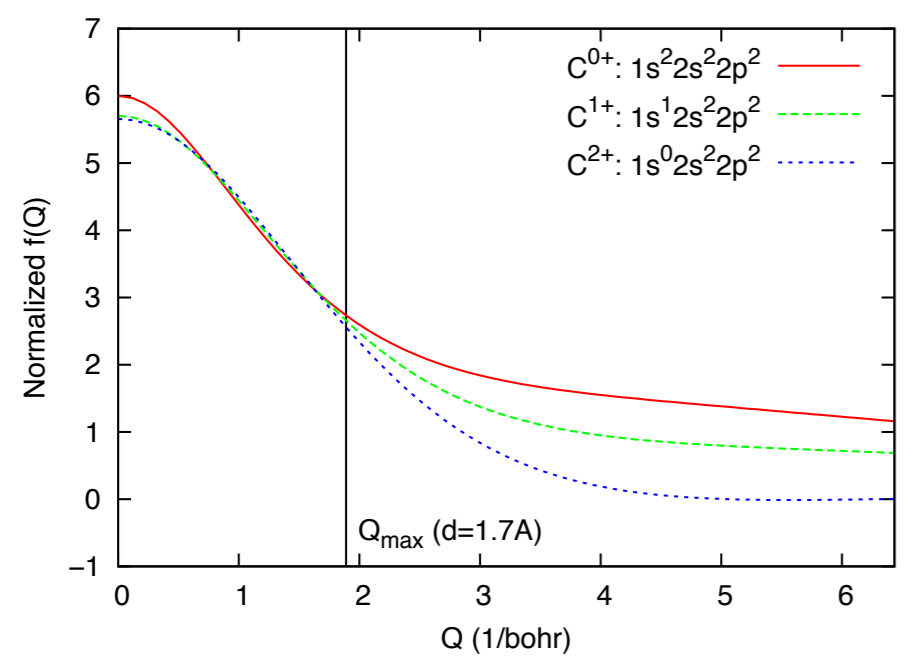
$$f''(\omega) = -\frac{\omega}{4\pi \alpha} \sigma_P(\omega)$$

C scattering from hollow atom

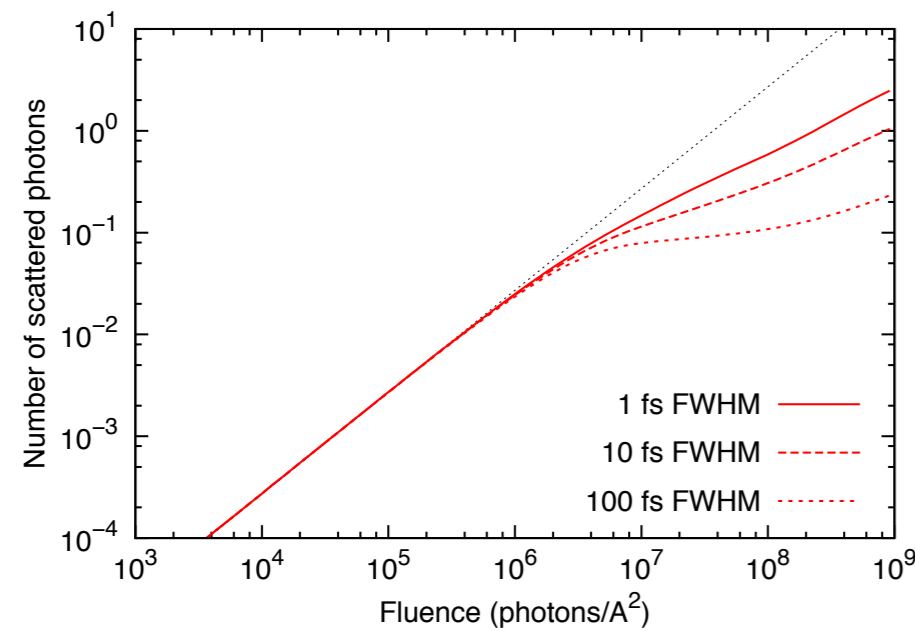
$1s^2 2s^2 2p^2$
N of config. = 27

One of the prospective applications of XFEL is single-shot imaging of individual macromolecules, which employs coherent X-ray scattering to determine the atomically resolved structure of non-crystallized biomolecules or other nanoparticles. During ultrashort and ultraintense X-ray pulses with an atomic scale wavelength, samples are subject to radiation damage, which may influence the quality of X-ray scattering patterns. Our numerical simulations of coherent X-ray scattering signals including electronic damage dynamics show that hollow-atom formation and the associated phenomenon of X-ray transparency or frustrated absorption play a crucial role in optimizing the strength and quality of single-shot X-ray scattering signals. The present results suggest that high-brightness attosecond XFELs would be ideal for single-shot imaging of individual macromolecules.

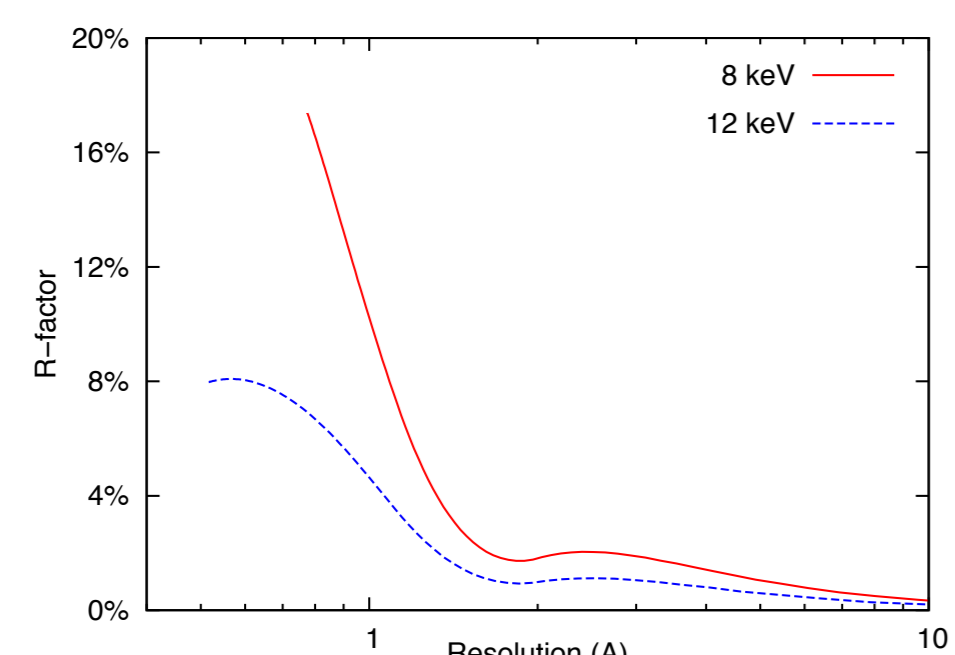
Normalized atomic form factor of carbon



Number of scattered photons vs. fluence (8 keV and resolution=1.7 Å)



R-factor vs. resolution (10⁷ photons/Å², 1 fs FWHM)



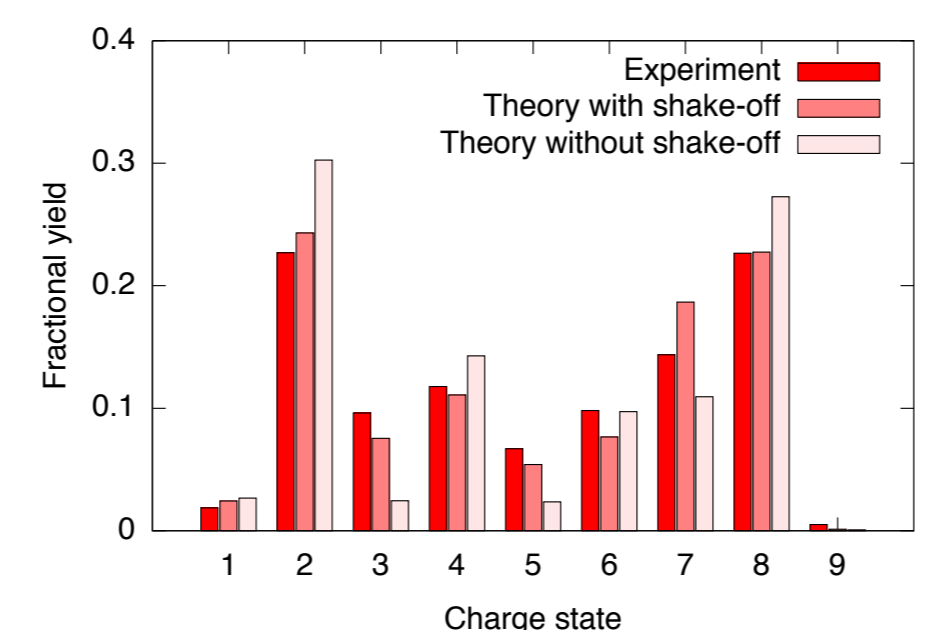
Son, Young & Santra, *Phys. Rev. A* **83**, 033402 (2011)

Ne nonlinear X-ray response

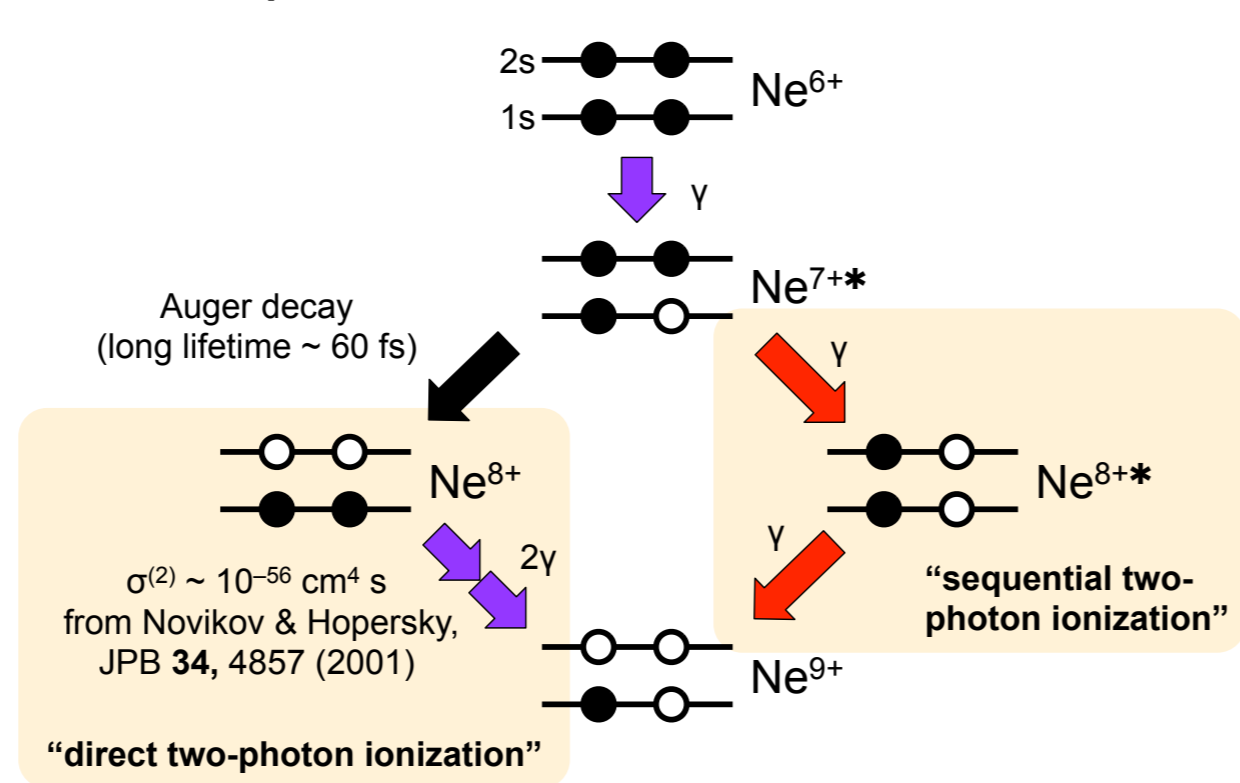
$1s^2 2s^2 2p^6$
N of config. = 63

The study and applications of nonlinear processes from the micro-wave to the ultraviolet frequencies are extensive, but not realized for X-ray until now. We present the first experimental evidence of nonlinear response in the X-ray regime. In theory, we have extended our model to include shake-off processes and to adapt the two-photon ionization cross section for the rate equation model. We have measured and analyzed quadratic dependence of Ne⁹⁺ production on intensity when the photon energy is below the K-shell threshold of Ne⁸⁺. Nonlinear response comes from two channels: direct two-photon ionization and sequential two-photon ionization with transient excited states competing with the Auger decay clock.

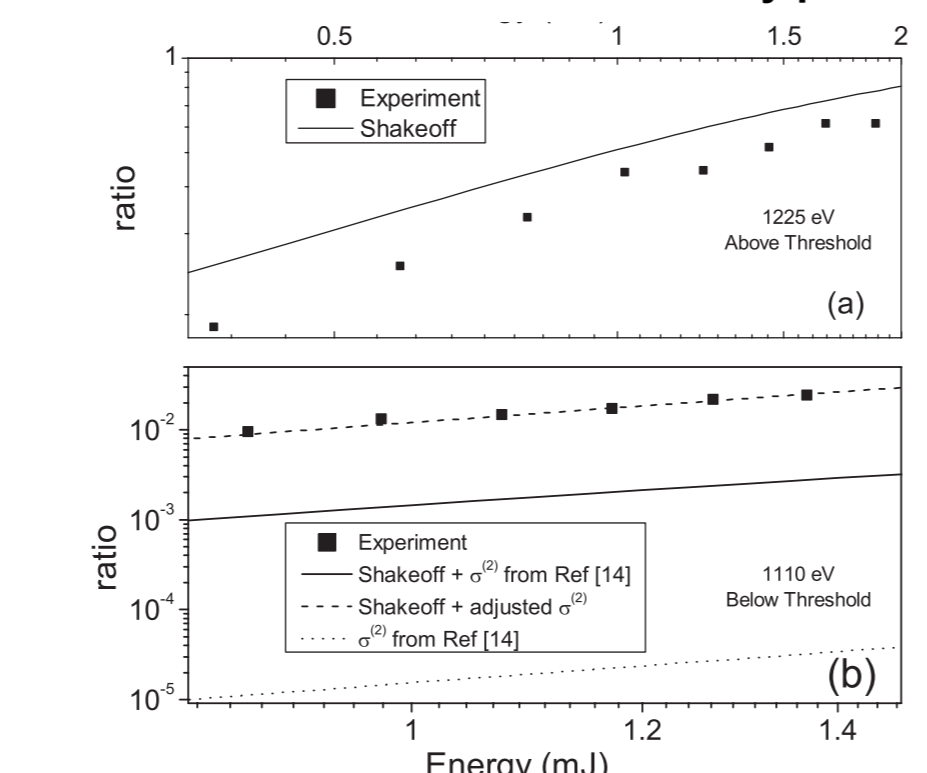
Charge state distribution produced by 1110 eV (1.27 mJ)



Two-photon ionization mechanisms at 1110 eV



The Ne⁹⁺/Ne⁸⁺ ratio as a function of X-ray pulse energy



Doumy *et al.*, *Phys. Rev. Lett.* **106**, 083002 (2011)

Fe MAD at high intensity

$1s^2 2s^2 2p^6 3s^2 3p^6 3d^6 4s^2$
N of config. = 194,481

MAD (multi-wavelength anomalous diffraction) is used to determine phase information in X-ray crystallography by employing resonant elastic X-ray scattering from heavy atoms. We have recently proposed that the MAD phasing method can be extended to structural determination of molecules under intense X-ray pulses. The scattering intensity (per unit solid angle) including electronic damage dynamics at high intensity (only heavy atoms scatter anomalously and undergo electronic damage) can be written as

$$\frac{dI(\mathbf{Q}, \omega)}{d\Omega} = C(\Omega) \int_{-\infty}^{\infty} dt J(t) \sum_i P_i(t) \left| F_H^0(\mathbf{Q}) + \sum_{j=1}^{N_H} f_{j, I_j}(\mathbf{Q}, \omega) e^{i\mathbf{Q}\cdot\mathbf{R}_j} \right|^2$$

$$f_{j, I_j}(\mathbf{Q}, \omega) = f_{j, I_j}^0(\mathbf{Q}) + f_{j, I_j}'(\omega) + i f_{j, I_j}''(\omega)$$

If we assume that there is only one kind of heavy atoms and changes of their configurations happen independently, the above equation can be reduced to a generalized Karle-Hendrickson equation,

$$\frac{dI(\mathbf{Q}, \omega)}{d\Omega} = FC(\Omega) \left[|F_H^0(\mathbf{Q})|^2 + |F_H^0(\mathbf{Q})|^2 \bar{a}(\mathbf{Q}, \omega) + |F_H^0(\mathbf{Q})| |F_H^0(\mathbf{Q})| b(\mathbf{Q}, \omega) \cos(\phi_H^0(\mathbf{Q}) - \phi_H^0(\mathbf{Q})) + |F_H^0(\mathbf{Q})| |F_H^0(\mathbf{Q})| c(\mathbf{Q}, \omega) \sin(\phi_H^0(\mathbf{Q}) - \phi_H^0(\mathbf{Q})) + N_H |f_H^0(\mathbf{Q})|^2 \{a(\mathbf{Q}, \omega) - \bar{a}(\mathbf{Q}, \omega)\} \right]$$

$$\bar{a}(\mathbf{Q}, \omega) = \frac{1}{|F_H^0(\mathbf{Q})|^2} \int_{-\infty}^{\infty} dt \frac{J(t)}{F} \left| \sum_{I_H} P_{I_H}(t) f_{H, I_H}(\mathbf{Q}, \omega) \right|^2$$

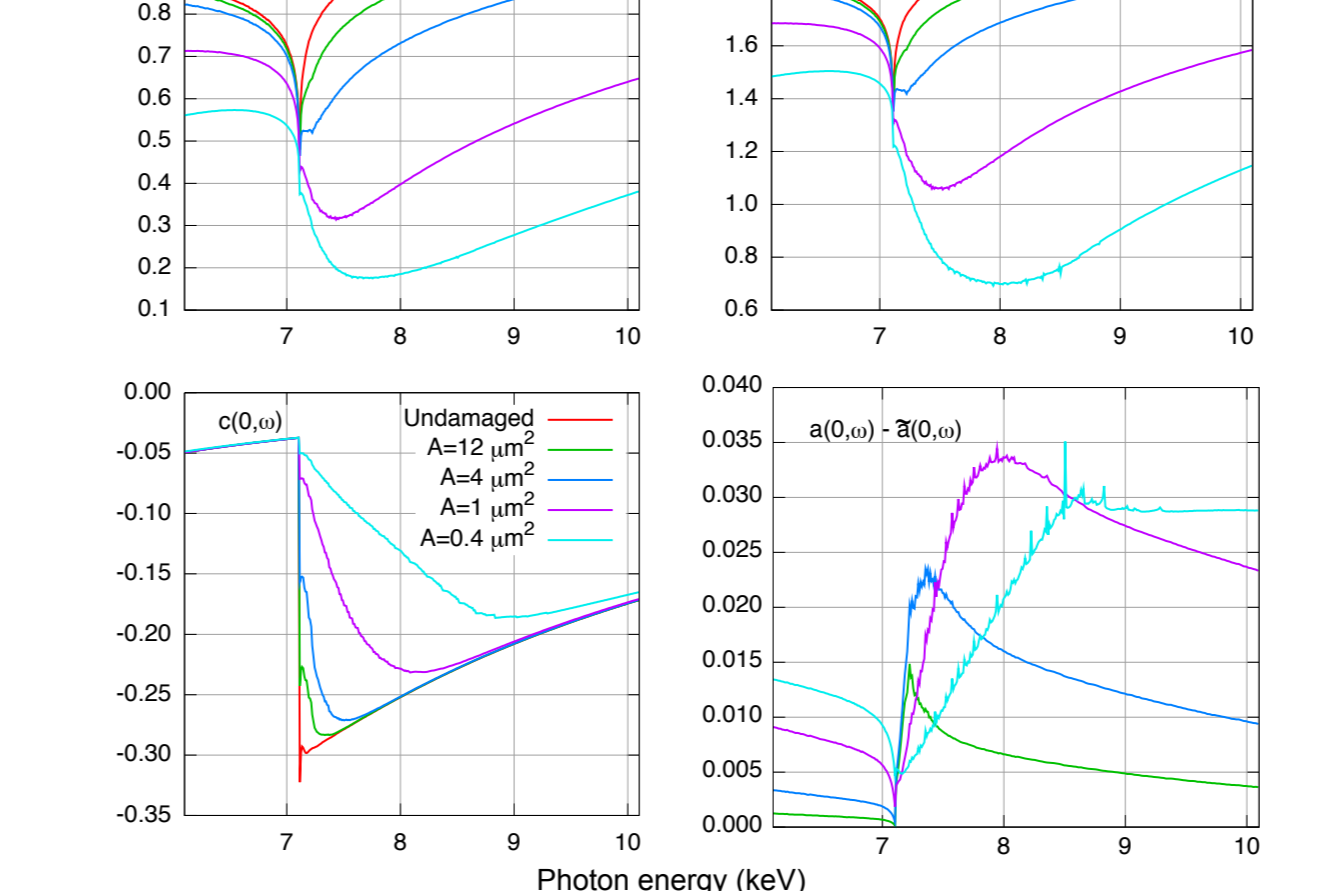
$$a(\mathbf{Q}, \omega) = \frac{1}{|F_H^0(\mathbf{Q})|^2} \sum_{I_H} P_{I_H} |f_{H, I_H}(\mathbf{Q}, \omega)|^2$$

$$b(\mathbf{Q}, \omega) = \frac{2}{|F_H^0(\mathbf{Q})|^2} \sum_{I_H} P_{I_H} \{ f_{H, I_H}^0(\mathbf{Q}) + f_{H, I_H}'(\omega) \}$$

$$c(\mathbf{Q}, \omega) = \frac{2}{|F_H^0(\mathbf{Q})|^2} \sum_{I_H} P_{I_H} f_{H, I_H}''(\omega)$$

$$F_H^0(\mathbf{Q}) = f_H^0(\mathbf{Q}) \sum_{j=1}^{N_H} e^{i\mathbf{Q}\cdot\mathbf{R}_j} \text{ for the ground-state config.}$$

Coefficients for the extended Karle-Hendrickson equation



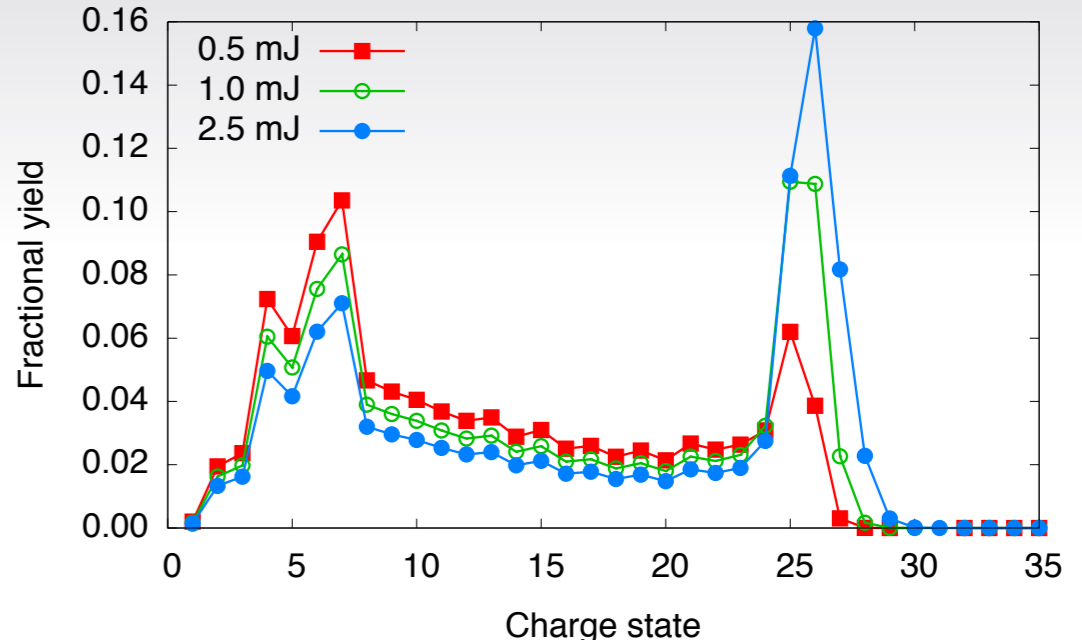
Collaboration with CFEL Coherent Imaging Son, Chapman & Santra (in preparation)

Xe role of high-E fluorescence

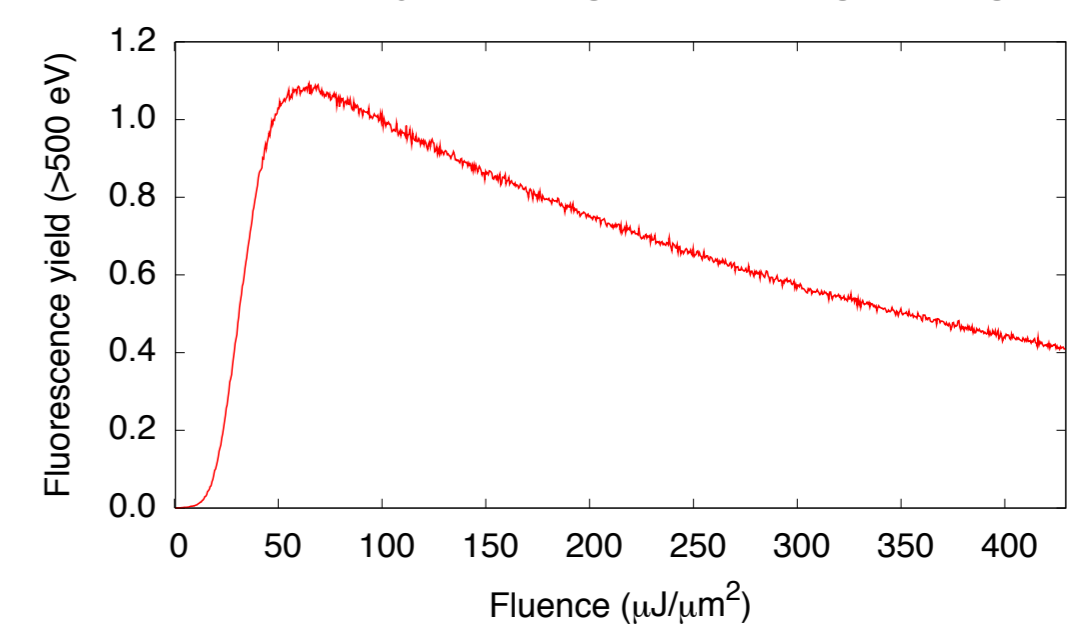
$1s^2 2s^2 2p^6 3s^2 3p^6 3d^{10} 4s^2 4p^6 4d^{10} 5s^2 5p^6$
N of config. = 1,120,581

In recent experiments, the CFEL-MPG-ASG team has measured charge state distribution and fluorescence spectra of Xe in coincidence. From theoretical point of view, this Xe problem is challenging because it has more than 1 million configurations and enormous numbers of processes are involved in electronic damage cascade. We have employed a Monte-Carlo approach to effectively solve the rate equation to attack this formidable task. Our numerical simulations show that charge state distribution of Xe is higher than expected from core-shell thresholds consideration. Also we have found an unusual nonlinear increase of high-energy fluorescence lines from 3p and 3d transitions as the fluence increases. From time-averaged population analysis of core-hole states, it can be shown that multiple-core-hole states of 3p and 3d subshells are responsible for these phenomena.

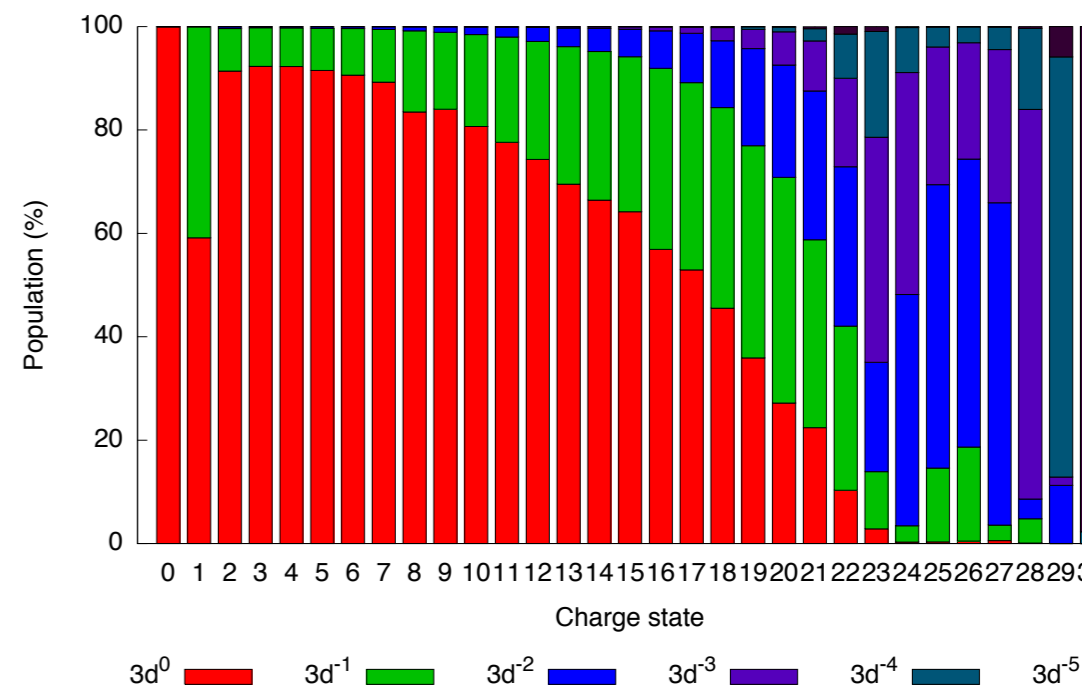
Charge state distribution produced by 1500 eV



Fluorescence yield integrated for high energies



Population analysis for 3d multiple-core-hole states



Collaboration with CFEL-MPG-ASG (Rolles, Rudenko & Ullrich)